Stoichiometry and Affinity of Nucleotide Binding to P-Glycoprotein during the Catalytic Cycle†

Qin Qu, Paula L. Russell, and Frances J. Sharom*

Guelph-Waterloo Centre for Graduate Work in Chemistry and Biochemistry, Department of Chemistry and Biochemistry, University of Guelph, Guelph, Ontario, Canada N1G 2W1

Received August 1, 2002; Revised Manuscript Received September 26, 2002

ABSTRACT: Drug transport mediated by P-glycoprotein (Pgp) is driven by hydrolysis of ATP at the two cytosolic nucleotide binding domains. However, little is currently known concerning the stoichiometry of nucleotide binding and how both stoichiometry and binding affinity change during the catalytic cycle of the transporter. To address this issue, we used fluorescence techniques to measure both the number of nucleotides bound to P-glycoprotein during various stages of the catalytic cycle and the affinity of nucleotide binding. Results showed that resting state P-glycoprotein bound two molecules of the fluorescent nucleotide derivative, 2′(3′)-*O*-(2,4,6-trinitrophenyl)adenosine 5′-triphosphate (TNP-ATP), whereas the vanadate-trapped transition state bound only one nucleotide molecule. Both resting and transition state P-glycoprotein showed similar affinity for TNP-ATP/TNP-ADP and unlabeled ATP/ADP. Following binding of various drugs, resting state P-glycoprotein displayed a higher affinity for nucleotides, up to 4-fold depending on the compound used. In contrast, the transition state showed substantially lower (up to 3-fold) nucleotide binding affinity when the drug binding site(s) is/are occupied. These results indicate that both nucleotide binding domains of P-glycoprotein are likely to be occupied with either ATP (or ADP) in the resting state and the transition state in the absence of transport substrates. Drugs alter the binding affinity to favor association of ATP with P-glycoprotein at the start of the catalytic cycle and release of ADP from the transition state following nucleotide hydrolysis.

The ABC superfamily of membrane transporters is one of the largest group of proteins represented in the genomes of humans (*1*), plants (*2*), and prokaryotes (*3*, *4*). Members of this protein superfamily are exporters or importers involved in a wide variety of important processes, including several human diseases (*5*, *6*), sterol absorption and excretion (*7*), multidrug resistance (MDR)[1] in human cancers (*8*), and antibiotic/drug resistance in aquatic organisms (*9*), bacteria (*10*), and yeast (*11*, *12*). Considerable effort is being expended to understand both the structure and the mechanism of action of proteins in this family, and two X-ray crystal structures of intact bacterial ABC transporters have appeared in the past year (*13*, *14*). While these models have provided stimulating insights into the architecture of ABC proteins, they are static structures and have shed little light on the details of the catalytic cycle and mechanism of action.

One important characteristic of ABC proteins is the presence of two cytosolic nucleotide binding (NB) domains, which hydrolyze ATP to provide the energy to drive substrate transport (*15*, *16*). Knowledge of the details of the catalytic cycle of ATP hydrolysis by the NB domains, and how this is coupled to substrate translocation, is essential to understanding the functioning of ABC proteins. The MDR1 multidrug efflux pump, known as P-glycoprotein (Pgp), is one of the most studied proteins in this superfamily. Expression of Pgp in human cancers is responsible for a major type of MDR (*17*−*19*), and the reversal of this drug resistance by chemical compounds known as modulators, or chemosensitizers, is an important clinical goal (*20*, *21*).

Pgp has been purified, and its ATPase activity has been extensively characterized (*22*−*24*). Senior and co-workers were the first to show that Pgp, like many other ATPases, can be trapped in an intermediate state partway through the catalytic cycle by reaction with vanadate (V_i) in the presence of ATP (*25*). After one round of ATP hydrolysis, P_i dissociates, and V_i takes its place, leading to trapping of the complex $ADP{\cdot}V_i{\cdot}M^{2+}$ (where M^{2+} is a divalent cation, such as Mg^{2+}, Mn^{2+}, or Co^{2+}) in one of the NB domains (see Figure 1). The conformation of the trapped state is thought to resemble that of the catalytic transition state. Vanadate trapping at one NB domain completely inhibited ATPase activity at both active sites, leading Senior and co-workers to propose an alternating sites model for ATP hydrolysis (*26*). In such a scheme, it is proposed that when one of the two NB domains is active, the other cannot enter the transition state, so that the two active sites take turns hydrolyzing ATP.

Senior et al. clearly showed that the N- and C-terminal halves of the Pgp molecule are functionally equivalent and

† This work was supported by a grant to F.J.S. from the National Cancer Institute of Canada, with funds provided by the Canadian Cancer Society.

* Corresponding author. Phone: (519) 824-4120 Ext. 2247. Fax: (519) 766-1499. E-mail: fsharom@uoguelph.ca.

[1] Abbreviations: ABC, ATP-binding cassette; CHAPS, 3-[(3-cholamidopropyl)-dimethylammonio]-1-propanesulfonate; MDR, multidrug resistance/resistant; MIANS, 2-(4′-maleimidylanilino) naphthalene-6-sulfonic acid; NB, nucleotide binding; Pgp, P-glycoprotein; TNP-ATP, 2′(3′)-*O*-(2,4,6-trinitrophenyl)adenosine 5′-triphosphate; TNP-ADP, 2′-(3′)-*O*-(2,4,6-trinitrophenyl)adenosine 5′-diphosphate.

10.1021/bi026555j CCC: $25.00
Published on Web 12/31/2002

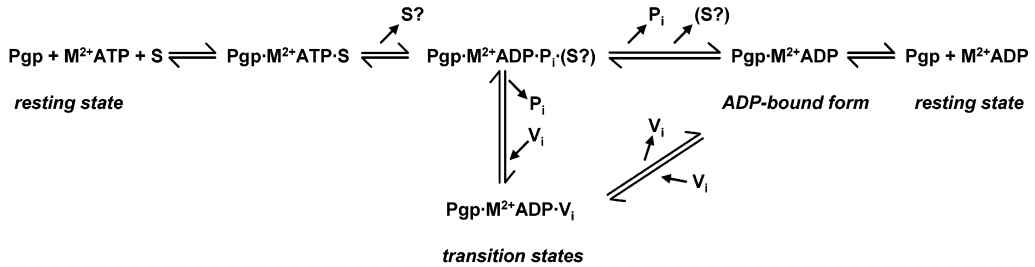

FIGURE 1: Scheme showing formation of the vanadate-trapped transition state of Pgp. Binding of drug substrate (S) and ATP, together with a divalent cation (Mg^{2+}, Mn^{2+}, or Co^{2+}) leads to formation of a ternary complex. Binding of ATP and substrate takes place in a random order. ATP hydrolysis to ADP and P_i leads to formation of the transition state complex. Dissociation of P_i, followed by association of orthovanadate, V_i, leads to formation of the vanadate-trapped transition state, which is proposed to have a similar conformation and properties to the native transition state. The vanadate-trapped transition state may also be formed by direct interaction of V_i with the ADP-bound form of Pgp. Slow dissociation of V_i from the vanadate-trapped transition state generates the ADP-bound form of Pgp, and the final step in the catalytic cycle, loss of ADP/divalent cation, regenerates the native state, which regains its ATPase activity. The step at which coupled substrate transport takes place is unclear. Davidson and co-workers found that the maltose permease had already lost its bound substrate by the time the vanadate-trapped transition state complex is formed and proposed a concerted transport mechanism whereby transport takes place during the ATP hydrolysis step (*54*). On the other hand, Ambudkar and co-workers have suggested a stepwise mechanism for substrate transport by Pgp, with drug dissociating from the vanadate-trapped transition state (shown on the scheme as S?) (*55*). Recent work in our laboratory strongly supports a concerted transport mechanism for Pgp (*56*).

that both are equally capable of binding and hydrolyzing nucleotide (*27*); however, the fractional occupancy of the two sites could not be determined. Thus, at the present time, the stoichiometry of nucleotide binding to Pgp is not known. Although the protein contains two NB domains, each of which can potentially bind nucleotide, it is possible that when one site is occupied with ATP, the other may be able to bind ADP but not ATP (as proposed by Druley et al., see ref *28*) or may be unable to bind nucleotide at all. Similarly, although vanadate trapping occurs nonselectively at either of the two active sites (*27*), it is not known whether vanadate-trapped transition state Pgp is able to bind nucleotide at the unoccupied NB domain. Knowledge of these details is essential for formulation of a detailed mechanism of action of the transporter and may invalidate certain currently proposed mechanistic schemes. Since Pgp displays constitutive ATPase activity in the absence of drug substrates (*23*), the full catalytic cycle of ATP hydrolysis can clearly proceed when the drug binding sites are unoccupied. However, since drug transport is driven by ATP hydrolysis, occupation of the drug binding sites may alter the affinity of the catalytic sites for nucleotides, depending on the stage of the catalytic cycle.

The present work was thus designed to answer some important questions about the stoichiometry and affinity of binding of nucleotides to Pgp at various stages of the catalytic cycle. Fluorescently labeled ATP was employed to determine the stoichiometry of binding to Pgp in both the resting state and the vanadate trapped transition state (see Figure 1). Using fluorescence quenching techniques, we also determined the affinity of resting and transition state Pgp for unmodified ATP and ADP and the effect of drug binding on the ATP binding affinity in both the resting state and the transition state.

MATERIALS AND METHODS

Materials. 2-(4′-maleimidylanilino) naphthalene-6-sulfonic acid (MIANS), 2′(3′)-*O*-(2,4,6-trinitrophenyl)adenosine 5′-triphosphate (TNP-ATP), and 2′(3′)-*O*-(2,4,6-trinitrophenyl)-adenosine 5′-diphosphate (TNP-ADP) were supplied by Molecular Probes (Eugene, OR). 3-[(3-Cholamidopropyl)-dimethylammonio]-1-propane-sulfonate (CHAPS), disodium ATP, sodium ADP, and sodium orthovanadate were purchased from Sigma Chemical Co. (St. Louis, MO). A stock solution of 100 mM sodium orthovanadate was prepared at pH 10, and polymeric species were degraded by boiling aliquots for 4 min before use.

Plasma Membrane Preparation and Pgp Purification. Plasma membrane vesicles were isolated from MDR CH^RB30 Chinese hamster ovary cells as described previously (*29*) and were stored at −70 °C for no more than 3 months before use. The plasma membrane vesicles were subjected to a two-step selective extraction to isolate Pgp. After treatment of the membrane vesicles with 25 mM CHAPS buffer and centrifugation, the resulting S_1 pellet was solubilized in 15 mM CHAPS buffer as described previously (*30*). Pgp was further purified from the soluble S_2 fraction by affinity chromatography on Concanavalin-A-Sepharose. The final purified Pgp preparation was 90−95% pure in 50 mM Tris-HCl/0.15 M NaCl/5 mM $MgCl_2$ buffer (pH 7.5) containing 2 mM CHAPS. Purified Pgp was kept on ice and used within 24 h. Purified Pgp was quantitated by the methods of either Peterson (*31*) or Bradford (*32*) using bovine serum albumin (crystallized and lyophilized, Sigma) as a standard.

Measurement of Pgp ATPase Activity. The Mg^{2+}-dependent ATPase activity of purified Pgp was determined by measuring the release of inorganic phosphate from ATP by a colorimetric method. As described previously (*23*, *33*), purified Pgp was incubated with assay buffer (50 mM Tris-HCl/0.15 M NaCl/5 mM $MgCl_2$, pH 7.5) in the presence of 1 mM ATP at 37 °C for various times, depending on the experiment; a 20 min incubation time was used for vanadate inhibition of Pgp ATPase activity, and 5 min was used for reactivation of Pgp ATPase activity (see below).

Determination of the Affinity and Stoichiometry of TNP-Labeled Nucleotide Binding to Resting and Transition State Pgp. For preparation of the Co^{2+}-trapped transition state of Pgp, 200 μg of purified protein in 2 mM CHAPS/50 mM Tris-HCl (pH 7.5) was incubated with 1 mM ATP, 5 mM $CoCl_2$, and 0.3 mM sodium orthovanadate in a final volume of 2.7 mL for 20 min at 37 °C. After incubation, the sample was eluted through a gel filtration column of Bio-Gel-P6 equilibrated with 2 mM CHAPS buffer to remove excess ATP, vanadate, $CoCl_2$, and inorganic phosphate.

Different fixed concentrations of resting or transition state Pgp (Pgp-V_i) were titrated at 22 °C with increasing concentrations of TNP-ATP or TNP-ADP. All fluorescence experiments were carried out in the presence of large unilamellar vesicles of asolectin (soybean phospholipids), prepared by extrusion through 100 nm polycarbonate filters (*34*, *35*), which were added to the Pgp solution at a final concentration of 0.5 mg/mL. A 500 μL aliquot of Pgp or Pgp-V_i was mixed with asolectin vesicles in a 0.5 cm quartz cuvette and titrated with 5 μL aliquots of TNP-labeled nucleotide in 2 mM CHAPS/50 mM Tris-HCl (pH 7.5) containing 0.5 mg/mL asolectin vesicles. The fluorescence emission was measured at 535 nm after excitation at 408 nm. A solution of 2 mM CHAPS/50 mM Tris-HCl (pH 7.5) containing 0.5 mg/mL asolectin vesicles was titrated as a control in all experiments. Titration data were fitting to the following equation describing interaction with a single type of binding site:

$$\Delta F = \frac{\Delta F_{max} \times [S]}{K_d + [S]}$$

where ΔF represents the change in fluorescence intensity following addition of TNP-labeled nucleotide at a concentration [*S*], ΔF_{max} is the maximum change in fluorescence intensity, and K_d is the dissociation constant. Fitting was performed using Sigma Plot (SPSS Inc., Chicago IL), and values for K_d and ΔF_{max} were extracted. The fitting errors for determination of ΔF_{max} were, on average, 5.2% for resting state Pgp and 3.8% for transition state Pgp.

Analysis of Stoichiometry of TNP-Labeled Nucleotide Binding. The stoichiometry of TNP-labeled nucleotide binding was determined by the approach of Huang et al. (*36*). First, the molar enhancement of fluorescence (ϕ), which is a measure of the hydrophobic nature of the nucleotide binding site, was calculated by determining the slope of a plot of ΔF_{max}/[Pgp], generated by performing TNP-ATP titrations at several different Pgp concentrations.

$$\phi = \frac{\Delta F_{max}}{[\text{Pgp}]}$$

The mass action plot of Dixon and Webb (*37*) was then applied to the fluorescence titration data for resting and transition state Pgp, and the binding stoichiometry of TNP-ATP was determined using the following equation:

$$\frac{r}{[\text{L}]_{free}} = \frac{n}{K_d} - \frac{r}{K_d}$$

where $[\text{L}]_{free}$ is the concentration of free ligand, *r* is the molar ratio of bound ligand to protein, K_d is the dissociation constant, and *n* is the stoichiometry of ligand binding. The concentration of bound ligand was estimated using the molar enhancement of fluorescence (ϕ), and the concentration of free ligand was calculated by subtracting the bound ligand concentration, $[\text{L}]_{bound}$, from the total ligand concentration. A plot of $r/[\text{L}]_{free}$ versus *r* gave a straight line with an *x*-intercept value of *n*, the binding stoichiometry.

Double and Single Labeling of Purified Pgp with MIANS. For measurement of nucleotide binding affinity to resting state Pgp by MIANS quenching, Pgp was labeled with MIANS at both NB domains (*30*). Purified Pgp (~200 μg) in a total volume of 1.5 mL in 2 mM CHAPS/50 mM Tris-HCl (pH 7.5) was incubated with 30 μM MIANS at 22 °C for 30 min in the dark. Protein labeled with MIANS at both NB domains (Pgp-2MIANS) was separated from unreacted MIANS by passing through a Bio-Gel P-6 gel filtration column equilibrated with 2 mM CHAPS buffer.

To prepare transition state Pgp, purified protein was singly labeled with MIANS at one NB domain, following trapping with V_i and Co^{2+} at the other NB domain, to give Pgp-V_i-MIANS (*38*). Purified Pgp (~200 μg) was incubated in a total volume of 1.5 mL of 2 mM CHAPS buffer containing 5 mM $CoCl_2$ at 37 °C for 20 min, in the presence of 1 mM ATP and 0.3 mM sodium orthovanadate. Unreacted species were removed by eluting the sample through a Bio-Gel-P6 gel filtration column equilibrated with 2 mM CHAPS buffer. The eluate was incubated with 30 μM MIANS at 22 °C for 30 min in the dark. To remove unreacted MIANS, the sample was passed through a Bio-Gel-P6 gel filtration column preequilibrated with 2 mM CHAPS buffer. Unlabeled Pgp was used as control for comparison to Pgp-2MIANS and Pgp-V_i-MIANS. The protein concentration of the various labeled Pgp samples was adjusted to between 50 and 100 μg/mL, depending on the experiment.

Measurement of Nucleotide Binding Affinity to Resting and Transition State Pgp by MIANS Quenching. Pgp-2MIANS and Pgp-V_i-MIANS were titrated with increasing concentrations of ATP or ADP as described previously (*30*). All experiments were carried out in the presence of 0.5 mg/mL asolectin vesicles. The working solutions of ATP or ADP were also prepared in 2 mM CHAPS buffer containing 0.5 mg/mL asolectin. Quenching experiments were performed by successively adding 5 μL aliquots of ATP or ADP working solution to 500 μL of MIANS-labeled Pgp in the absence or presence of drugs at a saturating concentration. The steady-state fluorescence of MIANS-labeled Pgp was measured at 420 nm for 20 s with excitation at 322 nm. Quenching of MIANS fluorescence at various nucleotide concentrations was fitted to the following equation:

$$\Delta F/F_0 \times 100 = \frac{(\Delta F_{max}/F_0 \times 100) \times [S]}{K_d + [S]}$$

where ($\Delta F/F_0 \times 100$) represents the percent change in fluorescence intensity relative to the initial value after addition of ATP or ADP at a concentration [*S*], ($\Delta F_{max}/F_0 \times 100$) is the maximum percent quenching of the fluorescence intensity that occurs upon saturation of the NB site, and K_d is the dissociation constant for binding of nucleotide to Pgp. Fitting was performed by regression analysis using SigmaPlot, and values of K_d and ΔF_{max} were extracted.

Fluorescence Measurements. Fluorescence spectra were recorded on a PTI Alphascan-2 spectrofluorimeter (Photon Technology International, London, ON Canada) with the cell holder thermostated at 22 °C. A 2 nm excitation and emission band-pass was used for all measurements. The emission spectra of labeled Pgps were corrected using a built-in automatic correction system. The measured fluorescence intensity was corrected for light scattering using controls containing unlabeled Pgp. In the fluorescence quenching titrations, the inner filter effect was corrected at both the excitation and the emission wavelengths as described previ-

ously (*30*, *39*, *40*), using the equation

$$F_{icor} = (F_i - B)(V_i/V_0)10^{0.5b(A_{lex}+A_{lem})}$$

where F_{icor} is the corrected value of the fluorescence intensity, F_i is the experimentally measured fluorescence intensity, B is the background fluorescence intensity caused by scattering, V_0 is the initial volume of the sample, V_i is the volume of the sample at a given point in the titration, b is the path length of the optical cell in cm, and $A_{\lambda ex}$ and $A_{\lambda em}$ are the absorbance of the sample at the excitation and emission wavelengths, respectively.

RESULTS

Interaction of Pgp with TNP-Labeled Nucleotides. We previously reported that the fluorescent nucleotides TNP-ATP and TNP-ADP interacted with the NB domains of purified Pgp (*41*). TNP-ATP was a classical competitive inhibitor of ATP hydrolysis, although it was a poor substrate, being hydrolyzed at ~5% of the rate measured for unmodified ATP. TNP-labeled nucleotides are only weakly fluorescent in aqueous solution. Their quantum yield is greatly enhanced upon transfer to a hydrophobic environment, such as the nucleotide binding site of a protein. TNP-ATP bound to resting state Pgp with a large saturable enhancement in the fluorescence emission, as shown by titration of a fixed concentration of Pgp with increasing amounts of TNP-ATP. Representative plots obtained at three different Pgp concentrations are shown in Figure 2A. Fitting of the titration curves to an equation for binding to a single type of site led to the estimation of two parameters (*41*), the dissociation constant (K_d), and the maximal fluorescence enhancement at saturating TNP-ATP, ΔF_{max}. The affinity of binding of TNP-ATP was ~50 μM, close to the value we reported previously (*41*). At the TNP-ATP and Pgp concentrations used in this study, Pgp will be substantially saturated with nucleotide, so the majority of Pgp molecules will have a nucleotide molecule bound at the completion of the titration with TNP-ATP. Increasing the Pgp concentration will thus lead to a proportional increase in the maximal fluorescence enhancement, ΔF_{max}. A plot of ΔF_{max} versus protein concentration gave a linear relationship, as expected. The slope of such a plot provides a value of the fluorescence yield, ϕ, which is defined as the fluorescence of TNP-ATP when bound to 1 μM protein ($\phi = \Delta F_{max}/[Pgp]$, see Materials and Methods). The value of ϕ for resting state Pgp was calculated to be 30.3 μM^{-1}.

Stoichiometry of Binding of TNP-Labeled Nucleotides to Resting State Pgp. ΔF_{max} and ϕ were used to generate values for $[TNP\text{-}ATP]_{bound}$, as described in Materials and Methods. Dixon plots of $r/[TNP\text{-}ATP]_{free}$ versus r for several protein concentrations were constructed and yielded straight lines converging close to $r = 2$. Two representative plots at different protein concentrations are shown in Figure 2B. Thus, the stoichiometry of TNP-ATP binding to resting state Pgp is 2, suggesting that both NB domains will normally be occupied with nucleotide.

Affinity and Stoichiometry of Binding of TNP-Labeled Nucleotides to Transition State Pgp. Transition state Pgp was prepared by trapping ADP·Vi·Co^{2+} in one of the NB domain active sites and removing the excess reagents by gel filtration chromatography. We previously showed that the vanadate-trapped protein prepared in this manner is extremely stable. Loss of vanadate and ADP from the active site, accompanied by reactivation of the ATPase activity, takes place only very slowly over a period of many hours. Less than 10% of the enzymatic activity had returned after a 3 h incubation at 22 °C (*42*). We verified that the transition state had almost complete (>95%) loss of ATPase activity before the start of each experiment, and ATPase activity was rechecked at the completion of each titration. TNP-ATP binding to Co^{2+}-trapped transition state Pgp also took place with an enhancement of the fluorescence emission (Figure 3A). The affinity of binding was similar to that seen for resting state Pgp (Table 1). However, the enhancement factor, ΔF, was about half that measured for TNP-ATP binding to resting state Pgp (compare Figure 2A with Figure 3A).

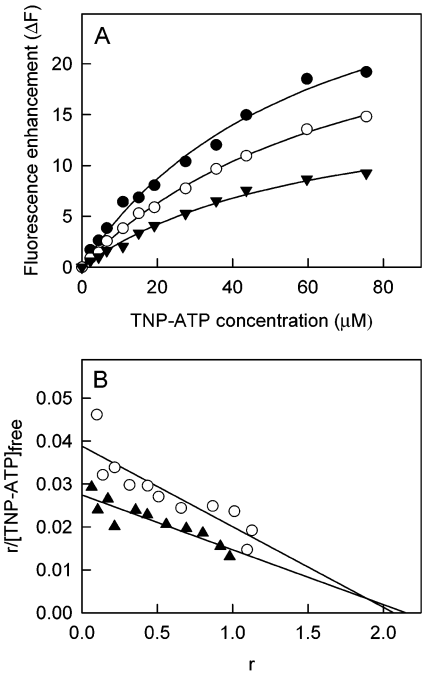

FIGURE 2: Affinity and stoichiometry of TNP-ATP binding to resting state Pgp. (A) TNP-ATP was titrated with purified Pgp at several different protein concentrations, and the fluorescence enhancement, ΔF, was measured. TNP-ATP was excited at 408 nm, and fluorescence emission was measured at 535 nm. Titrations are shown for three Pgp concentrations: ● = 1.13 μM; ○ = 0.87 μM; and ▼ = 0.60 μM. Titration curves were individually fitted to an equation describing binding to a single affinity site (solid lines), and values for the dissociation constant, K_d, and the maximum fluorescence enhancement, ΔF_{max}, were estimated. (B) Dixon plots used to determine the stoichiometry of TNP-ATP binding to resting state Pgp. Two representative plots at different Pgp concentrations are shown; ○ = 0.87 μM and ▼ = 0.60 μM. Data were fitted to the equation of Dixon and Webb (see Materials and Methods) using linear regression.

As with resting state Pgp, the value of ΔF_{max} was linearly proportional to the concentration of trapped Pgp. A ΔF_{max} value of ~8 was obtained at a protein concentration of 0.5 μM, and the value of ϕ was calculated to be 14.9 μM^{-1}, about half that seen for resting state Pgp. Dixon plots of $r/[TNP\text{-}ATP_{free}]$ versus r for several protein concentrations yielded straight lines converging close to $r = 1$; two representative plots at different protein concentrations are shown in Figure 3B. Thus, transition state Pgp can bind one molecule of TNP-ATP at the empty active site, with a similar binding affinity to that observed for resting state Pgp.

Table 1: Affinity of Resting and Transition State Pgp for Binding Nucleotides

	K_d (mM)[a]			K_d (μM)[a]	
	resting state Pgp-2MIANS	transition state Pgp-V_i-MIANS		resting state Pgp	transition state Pgp-V_i
ATP	0.404 ± 0.042	0.433 ± 0.026	TNP-ATP	50.3 ± 5.7	47.6 ± 4.1
ADP	0.407 ± 0.033	0.479 ± 0.063	TNP-ADP	41.9 ± 2.2	38.8 ± 3.1

[a] Three independent experiments were carried out for determination of each value of K_d, with different preparations of Pgp and Pgp-V_i-MIANS in each case. Mean ±SEM are indicated.

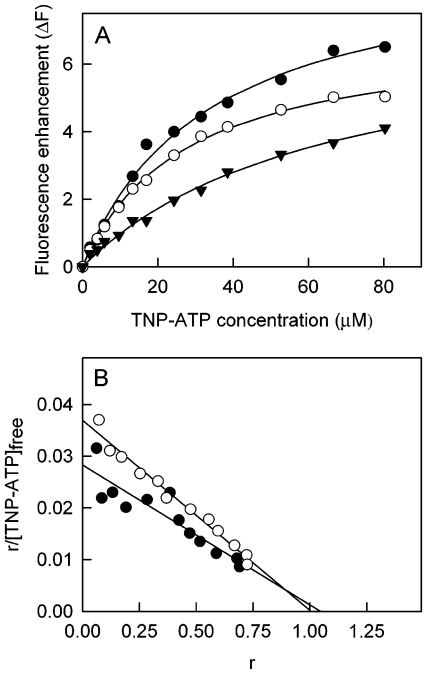

FIGURE 3: Affinity and stoichiometry of TNP-ATP binding to transition state Pgp trapped with ADP·V_i·Co^{2+}. (A) TNP-ATP was titrated with purified transition state Pgp at several different protein concentrations, and the fluorescence enhancement, ΔF, was measured at each nucleotide concentration. TNP-ATP was excited at 408 nm, and fluorescence emission was measured at 535 nm. Titrations are shown for three Pgp concentrations: ● = 0.633 μM; ○ = 0.467 μM; and ▼ = 0.411 μM. Titration curves were individually fitted to an equation describing binding to a single affinity site (solid lines), and values for the dissociation constant, K_d, and the maximum fluorescence enhancement, ΔF_{max}, were estimated. (B) Dixon plots used to determine the stoichiometry of TNP-ATP binding to transition state Pgp. Two representative plots at different Pgp concentrations are shown: ● = 0.633 μM and ○ = 467 μM. Data were fitted to the Dixon equation (see Materials and Methods) using linear regression.

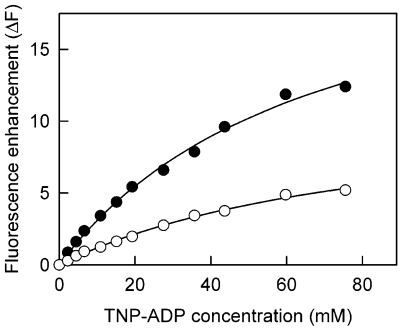

FIGURE 4: Binding of TNP-ADP to resting and transition state Pgp. TNP-ADP was titrated with purified resting state (●) and transition state Pgp (○), and the fluorescence enhancement, ΔF, was measured at each nucleotide concentration. TNP-ADP was excited at 408 nm, and fluorescence emission was measured at 535 nm. Titration curves were individually fitted to an equation describing binding to a single affinity site (solid lines), and values for the dissociation constant, K_d, and the maximum fluorescence enhancement, ΔF_{max}, were estimated.

Both resting and transition state Pgp bound TNP-ADP with saturable enhancement of the fluorescence emission (Figure 4). These results indicate that the transition state can also bind TNP-ADP. Resting and transition state Pgp bound TNP-ADP with similar affinities (Table 1). TNP-ADP bound with a slightly higher affinity (K_d close to 40 μM) as compared to TNP-ATP (Table 1).

Affinity of Binding of ATP and ADP to Resting and Transition State Pgp. We previously developed a fluorescence quenching technique for quantitation of the affinity of binding of unmodified nucleotides to purified Pgp under equilibrium conditions (*30*). Labeling of purified Pgp with the sulfhydryl-reactive fluorophore MIANS and other reagents results in covalent modification of Cys 428 and Cys 1071 (*43*) within the Walker A motifs of the NB domains (Pgp-2MIANS). MIANS-labeled Pgp binds drugs and nucleotides with normal affinity, as shown by photoaffinity labeling and fluorescence studies (*30*, *41*, *44*). Its ATPase activity is blocked, likely by a steric effect; this is an advantage when dissecting out the conformational changes associated with the catalytic cycle since the protein can be loaded with drug and ATP but will not progress further.

Titration of the MIANS-labeled protein with increasing concentrations of nucleotide led to concentration-dependent saturable quenching of the MIANS fluorescence, which was fitted to a binding equation for estimation of the dissociation constant, K_d, for nucleotide binding. Both ATP and ADP bound to resting state Pgp with an almost identical K_d value of around 0.4 mM (Figure 5A, Table 1), which is similar to the K_M measured for hydrolysis of ATP by the purified protein in detergent solution (*23*). The measured K_M for ATP from the kinetics of transport of a rhodamine dye by Pgp reconstituted into lipid bilayer vesicles is also comparable (*45*). Transition state Pgp, stably trapped using vanadate, ATP, and Co^{2+}, was labeled with MIANS at the Walker A Cys residue in the unoccupied NB domain to give Pgp-V_i-MIANS, as described earlier (*38*). Titration with ATP and ADP led to fluorescence quenching, again clearly indicating that the transition state can indeed bind both nucleotides at the unoccupied active site (Figure 5B). Thus, ATP and ADP bind to Pgp with comparable affinity in both the resting state and the vanadate trapped transition state.

Effect of Occupation of the Drug Binding Site(s) on Nucleotide Binding Affinity. Previous work in our laboratory showed that binding of nucleotides and drugs to Pgp occurs independently; in other words, occupation of the drug and nucleotide binding sites occurs in a random order (*30*). However, it is not known whether binding of drug affects the affinity of ATP binding. Clearly, both NB sites must be

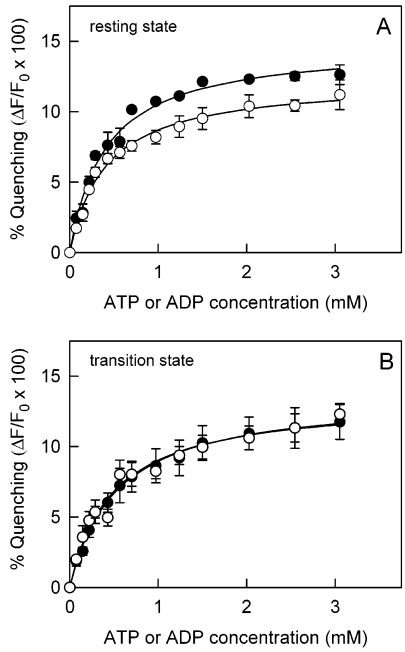

FIGURE 5: Affinity of Pgp for binding ATP (●) and ADP (○), as determined by quenching of MIANS-labeled Pgp. (A) Resting state Pgp labeled at two active site Cys residues (Pgp-2MIANS). (B) Vanadate-trapped transition state Pgp labeled at one active site Cys residue (Pgp-V_i-MIANS). Labeled Pgp was titrated with nucleotide, and the fluorescence quenching at 420 nm was determined at each concentration, following excitation at 322 nm. Titration curves were individually fitted to an equation describing binding to a single affinity site (solid lines), and values for the dissociation constant, K_d, were estimated. Data are presented as the mean ±SEM for triplicate determinations. Where error bars are not visible, they are contained within the symbols.

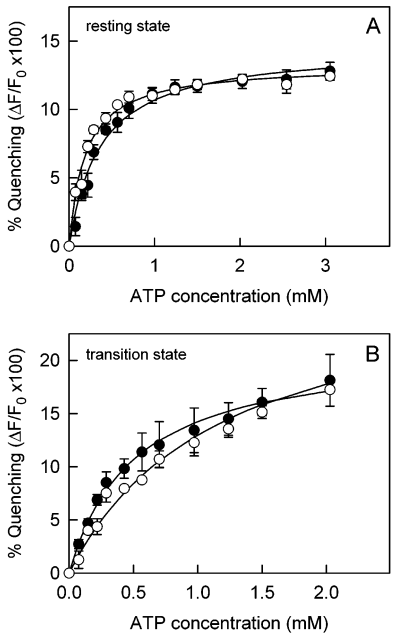

FIGURE 6: Affinity of Pgp for binding ATP in the presence (○) or absence (●) of the transport substrate vinblastine. (A) Resting state Pgp labeled at two active site Cys residues (Pgp-2MIANS). (B) Vanadate-trapped transition state Pgp labeled at one active site Cys residue (Pgp-V_i-MIANS). Labeled Pgp was incubated with 10 μM vinblastine, then titrated with ATP. After each addition, the fluorescence quenching at 420 nm was determined following excitation at 322 nm. Titration curves were individually fitted to an equation describing binding to a single affinity site (solid lines), and values for the dissociation constant, K_d, were estimated. Data are presented as the mean ±SEM for triplicate determinations. Where error bars are not visible, they are contained within the symbols.

occupied to initiate the transport process, and binding of many transport substrates and modulators greatly stimulates the hydrolysis of ATP (typically ranging from 20−400%; refs *23*, *46*, *47*), which is absolutely required for drug transport to take place. To determine whether drug binding to Pgp affects the affinity of ATP binding, resting and transition state Pgp were labeled with MIANS, incubated in the absence and presence of various drugs and modulators, and the affinity of ATP binding was measured by fluorescence quenching titration. The results shown in Figure 6A indicate that ATP binds to resting state Pgp with modestly increased affinity (2-fold higher; see Table 2) when the drug binding site is occupied by vinblastine. In contrast, in the stable transition state trapped with vanadate and Co^{2+}, binding of vinblastine resulted in a substantial decrease (2.4-fold; see Table 2) in the affinity of ATP binding. The drug substrate colchicine, and the modulators verapamil and cyclosporin A, produced comparable results (Table 2). In all cases, there was an increase in ATP binding affinity in resting state Pgp when the drug binding sites were occupied, ranging from an increase of ~4-fold for colchicine to 45% higher for verapamil. In contrast, the transition state displayed a consistent decrease in ATP binding affinity when the drug binding site was occupied, ranging from a decrease of over 3-fold for colchicine to 45% lower in the case of cyclosporin A.

Table 2: Affinity of Resting and Transition State Pgp for Binding ATP in the Presence of Drugs and Modulators[a]

	Fold Change in K_d	
	resting state Pgp-2MIANS	transition state Pgp-V_i-MIANS
colchicine (50 μM)	0.28 ± 0.10	3.37 ± 0.91
vinblastine (10 μM)	0.51 ± 0.074	2.35 ± 0.39
verapamil (30 μM)	0.69 ± 0.083	1.70 ± 0.35
cyclosporin A (4 μM)	0.43 ± 0.063	1.45 ± 0.16

[a] Separate experiments were carried for each drug or modulator, using a different Pgp preparation. In each experiment, Pgp-2MIANS and Pgp-V_i-MIANS (prepared from the same batch of Pgp) were titrated first with ATP, then with ATP in the presence of drug or modulator at concentrations close to saturating, except for colchicine (*30*, *44*). Different batches of Pgp show variations in the absolute value of the K_d for ATP binding. To allow meaningful comparison between the ATP binding affinity in the absence and presence of drug, the fold change in the value of K_d was calculated as (K_d + drug)/(K_d − drug). Three experiments were carried out for each drug or modulator, and the mean ±SEM values are given.

DISCUSSION

Many details of the catalytic cycle of ATP hydrolysis by Pgp remain unexplored. In particular, the stoichiometry and affinity of nucleotide binding during various stages of the catalytic cycle have not been addressed, yet such information is critical to building models of how the ATPase function of Pgp drives drug transport. In the present study, we have addressed this issue directly, using purified Pgp in either the resting state or the vanadate-trapped transition state. Various fluorescence techniques have been used to determine the nucleotide binding properties of these two states, either in the absence of drug substrates, which would represent the constitutive ATP hydrolysis cycle of Pgp, or in the presence

of drug substrates, which reflects the full transport cycle of the efflux pump.

Some previous studies have attempted to determine the properties of transition state Pgp using photoaffinity labeling. It is worth pointing out differences in the methodology used for the latter as compared to those used to generate the data in the present work. First, purified Pgp was used for all experiments rather than crude membrane preparations or partially purified protein. The preparation used in this work has high ATPase activity and has been well-characterized. Second, we prepared transition state Pgp using Co^{2+}, which is known to result in a highly stable vanadate-trapped state (*25*). Stoichiometric trapping was verified by almost complete loss of ATPase activity, and the length of time the protein stayed in the trapped state was characterized via measurement of the return of ATPase activity (*42*). Even after 3 h, only ~10% of the trapped state had regained its enzymatic activity by loss of ADP and V_i. In contrast, the transition state trapped with Mg^{2+} reactivated relatively quickly at 37 °C (*38*), so that a substantial fraction of the protein will exit the transition state over experimental times as short as 20 min. Third, trapped transition state Pgp was separated from the excess reagents used for trapping and studied in isolation. In photoaffinity labeling studies, excess vanadate, labeled azido-ATP, P_i, and high concentrations of unlabeled ATP are all present during the analysis, limiting its flexibility (for example, the NB domains will be fully saturated with nucleotide).

Stoichiometry experiments using binding of TNP-ATP showed that two molecules of nucleotide bound to resting state Pgp, whereas one molecule bound to the vanadate trapped transition state, with similar K_d values. Thus, both NB domains of resting state Pgp each bind nucleotide, and the unoccupied NB domain of the transition state is indeed able to bind nucleotide, with normal affinity. In this study, we show that unmodified ADP and ATP also bind to resting and transition state Pgp with a similar affinity of 0.4−0.5 mM. We estimate that the NB domains of Pgp will be ~80% saturated with nucleotide at typical intracellular concentrations of ATP (the cytosolic ATP concentration is generally 1.5−2 mM, and the ADP concentration ~0.1% of that). Taken together, these results indicate that, in the absence of transport substrates, the NB domains of Pgp are likely to be close to fully occupied with ATP in both the resting and the transition state. This proposal is in agreement with the findings of Druley et al. using the monoclonal antibody UIC2, which appears to be able to distinguish between two different Pgp conformations, one bound to nucleotide and one with empty catalytic sites (*28*). The low reactivity state is proposed to correspond to the ATP-bound conformation, the high reactivity state to the state with empty NB domains. In MDR1-expressing intact cells, most (>80%) of the cells appear to be in the low UIC2 reactivity state, suggesting that they have ATP bound to them.

Druley et al. found that the apparent Hill number for the nucleotide-dependent decrease in UIC2 reactivity in permeabilized cells was around 1 in the presence of nonhydrolyzable ATP analogues but close to 2 in the presence of ATP (*28*). They interpreted this as indicating that addition of ATP to the transporter results in ATP being bound at one active site, and ADP at the other, presumably after one hydrolysis turnover event. They proposed that Pgp can bind one molecule of ATP and one molecule of ADP simultaneously but not two molecules of ATP. This conclusion is clearly at odds with our results. A recent study of the NB cassettes of an archaeal ABC protein found that nonhydrolyzable ATP analogues did not accurately mimic ATP (*48*) and recommended that they be used with caution. It should also be noted that the UIC2 binding data is indirect in nature and not strictly kinetic in form, and so the application of kinetic analysis to give apparent Hill coefficients might produce parameters that are difficult to interpret.

Sauna et al. reported that vanadate-trapped Pgp (~80% pure) showed an apparently greatly reduced affinity for TNP-ATP (*49*). In fact, Sauna et al. did not measure binding affinity per se, only the fluorescence enhancement after adding a single concentration of TNP-ATP to partially purified Pgp. As compared to resting state Pgp, TNP-ATP fluorescence enhancement was ~30−35% for the vanadate trapped state, whether it was generated via hydrolysis of ATP or directly from ADP (*49*). In the present work, we show that the TNP-ATP binding affinity of transition state Pgp is in fact almost identical to that of resting state protein, but the fluorescence enhancement for binding to the transition state is about half that of the resting state, thus providing one explanation for their observation of lower fluorescence emission.

Sauna and Ambudkar showed that 8-azido-ADP bound to resting state Pgp with similar affinity to 8-azido-ATP (*49*), which provides support for our conclusions that ATP and ADP bind with similar affinity. On the other hand, they reported that photolabeling of Pgp with 8-azido-ATP was drastically lower in the vanadate-trapped transition state and proposed that the affinity of nucleotide binding to the transition state was reduced by at least 30-fold (*50*). Our results clearly show that isolated purified transition state Pgp binds nucleotide with unchanged affinity. We suggest that an observed reduction in photolabeling efficiency cannot be interpreted as a reduction in binding affinity. Protease sensitivity experiments have shown that vanadate-trapped transition state Pgp has a dramatically different conformation from the resting state (*51*, *52*), and we have recently confirmed and extended this observation using fluorescence quenching experiments (P. Russell and F. J. Sharom, unpublished data). Since photolabeling efficiency must clearly be dependent on protein conformation, it seems likely that the lack of nucleotide photolabeling observed for the transition state (*50*) reflects a change in the reaction efficiency of the photoprobe rather than a reduction in nucleotide binding affinity. Such an effect was pointed out several years ago by Sankaran et al. (*53*). They reported that while 2-azido-ATP and 8-azido-ATP bound to Pgp with similar affinities, only 8-azido-ATP showed highly efficient photolabeling of the transition state complex. No photolabeling at all was detected using the 2-azido analogue, likely as a result of lack of suitably positioned amino acids side chains in the active site of the transition state, yet it was able to efficiently label resting state Pgp. Ambudkar and coworkers also proposed, on the basis of photolabeling experiments, that the vanadate-trapped transition state essentially does not bind substrate because of a greatly lowered binding affinity. Yet we recently reported that the fluorescent drug substrate, Hoechst 3342, bound to purified transition state

Pgp with comparable affinity to the resting state, and we were able to use resonance energy transfer to estimate the location of the drug binding site within the protein (*42*). Photolabeling is thus not a suitable technique for quantitation of alterations in binding affinity where changes in protein conformation also take place since the efficiency of labeling of the two different protein conformations is likely to be different.

We found that occupation of the substrate binding sites by several different drugs and modulators increased the nucleotide binding affinity of the transporter in the resting state but had the opposite effect in the transition state. Thus, drugs alter the binding affinity to favor association of ATP with P-glycoprotein at the start of the catalytic cycle and release of ADP from the transition state following nucleotide hydrolysis. We previously showed that binding of drug and ATP takes place independently, so that ATP binding could precede, follow, or accompany drug binding (*30*). The results of the present work suggest that ATP binding is favored by occupation of the drug binding site, so that the presence of both transported substrate and ATP would be expected to promote both the transport cycle and the ATPase catalytic cycle. Once again, this is contrast to the work of Druley et al., who postulated (based on UIC2 reactivity studies in permeabilized intact cells) that binding of the drug vinblastine favors nucleotide debinding (*28*). Promotion of ATP dissociation prior to ATP hydrolysis seems counterintuitive to the operation of the transport cycle of Pgp. The changes in Pgp nucleotide binding affinity noted in the presence of drugs and modulators are not large; however, in combination they would have the effect of driving the catalytic cycle in the direction of ATP binding to the resting state and ADP dissociation from the transition state.

REFERENCES

1. Dean, M., Rzhetsky, A., and Allikmets, R. (2001) *Genome Res. 11*, 1156−1166.
2. Sánchez-Fernández, R., Davies, T. G. E., Coleman, J. O. D., and Rea, P. A. (2001) *J. Biol. Chem. 276*, 30231−30244.
3. Dassa, E., and Schneider, E. (2001) *Res. Microbiol. 152*, 203.
4. Hosie, A. H. F., and Poole, P. S. (2001) *Res. Microbiol. 152*, 259−270.
5. Borst, P., and Oude Elferink, R. P. (2002) *Annu. Rev. Biochem. 71*, 537−592.
6. Gottesman, M. M., and Ambudkar, S. V. (2001) *J. Bioenerg. Biomembr. 33*, 453−458.
7. Ordovas, J. M., and Tai, E. S. (2002) *Nutr. Rev. 60*, 30−33.
8. Litman, T., Druley, T. E., Stein, W. D., and Bates, S. E. (2001) *Cell. Mol. Life Sci. 58*, 931−959.
9. Bard, S. M. (2000) *Aquatic. Toxicol. 48*, 357−389.
10. Higgins, C. F. (2001) *Res. Microbiol. 152*, 205−210.
11. Wolfger, H., Mamnun, Y. M., and Kuchler, K. (2001) *Res. Microbiol. 152*, 375−389.
12. Del Sorbo, G., Schoonbeek, H. J., and De Waard, M. A. (2000) *Fungal Genet. Biol. 30*, 1−15.
13. Chang, G., and Roth, C. B. (2001) *Science 293*, 1793−1800.
14. Locher, K. P., Lee, A. T., and Rees, D. C. (2002) *Science 296*, 1091−1098.
15. Holland, I. B., and Blight, M. A. (1999) *J. Mol. Biol. 293*, 381−399.
16. Schneider, E., and Hunke, S. (1998) *FEMS Microbiol. Rev. 22*, 1−20.
17. Kerbel, R. S. (2001) *Cancer Metastasis Rev. 20*, 1−2.
18. Goldie, J. H. (2001) *Cancer Metastasis Rev. 20*, 63−68.
19. Sonneveld, P. (2000) *J. Intern. Med. 247*, 521−534.
20. Sikic, B. I. (1997) *Semin. Hematol. 34*, 40−47.
21. Dantzig, A. H., Law, K. L., Cao, J., and Starling, J. J. (2001) *Curr. Med. Chem. 8*, 39−50.
22. Urbatsch, I. L., al-Shawi, M. K., and Senior, A. E. (1994) *Biochemistry 33*, 7069−7076.
23. Sharom, F. J., Yu, X., Chu, J. W. K., and Doige, C. A. (1995) *Biochem. J. 308*, 381−390.
24. Shapiro, A. B., and Ling, V. (1994) *J. Biol. Chem. 269*, 3745−3754.
25. Urbatsch, I. L., Sankaran, B., Weber, J., and Senior, A. E. (1995) *J. Biol. Chem. 270*, 19383−19390.
26. Senior, A. E., al-Shawi, M. K., and Urbatsch, I. L. (1995) *FEBS Lett. 377*, 285−289.
27. Urbatsch, I. L., Sankaran, B., Bhagat, S., and Senior, A. E. (1995) *J. Biol. Chem. 270*, 26956−26961.
28. Druley, T. E., Stein, W. D., and Roninson, I. B. (2001) *Biochemistry 40*, 4312−4322.
29. Doige, C. A., and Sharom, F. J. (1991) *Protein Expr. Purif. 2*, 256−265.
30. Liu, R., and Sharom, F. J. (1996) *Biochemistry 35*, 11865−11873.
31. Peterson, G. L. (1977) *Anal. Biochem. 83*, 346−356.
32. Bradford, M. M. (1976) *Anal. Biochem. 72*, 248−254.
33. Doige, C. A., Yu, X., and Sharom, F. J. (1992) *Biochim. Biophys. Acta 1109*, 149−160.
34. Mayer, L. D., Bally, M. B., Hope, M. J., and Cullis, P. R. (1985) *Biochim. Biophys. Acta 816*, 294−302.
35. Mayer, L. D., Hope, M. J., and Cullis, P. R. (1986) *Biochim. Biophys. Acta 858*, 161−168.
36. Huang, S. G., Weisshart, K., and Fanning, E. (1998) *Biochemistry 37*, 15336−15344.
37. Dixon, M., and Webb, E. C. (1979) *Enzymes*, 3rd ed., Longman Group, London.
38. Qu, Q., and Sharom, F. J. (2001) *Biochemistry 40*, 1413−1422.
39. Lakowicz, J. R. (1999) *Principles of Fluorescence Spectroscopy*, 2nd ed., Kluwer Academic Publishers, New York.
40. Parker, C. A. (1968) *Photoluminescence of Solutions*, Elsevier Publishing Co., Amsterdam.
41. Liu, R., and Sharom, F. J. (1997) *Biochemistry 36*, 2836−2843.
42. Qu, Q., and Sharom, F. J. (2002) *Biochemistry 41*, 4744−4752.
43. Loo, T. W., and Clarke, D. M. (1995) *J. Biol. Chem. 270*, 22957−22961.
44. Sharom, F. J., Lu, P., Liu, R., and Yu, X. (1998) *Biochem. J. 333*, 621−630.
45. Lu, P., Liu, R., and Sharom, F. J. (2001) *Eur. J. Biochem. 268*, 1687−1697.
46. Sharom, F. J. (1997) *J. Membr. Biol. 160*, 161−175.
47. Sharom, F. J., Yu, X., DiDiodato, G., and Chu, J. W. K. (1996) *Biochem. J. 320*, 421−428.
48. Moody, J. E., Millen, L., Binns, D., Hunt, J. F., and Thomas, P. J. (2002) *J. Biol. Chem. 277*, 21111−21114.
49. Sauna, Z. E., Smith, M. M., Müller, M., and Ambudkar, S. V. (2001) *J. Biol. Chem. 276*, 21199−21208.
50. Sauna, Z. E., and Ambudkar, S. V. (2001) *J. Biol. Chem. 276*, 11653−11661.
51. Julien, M., and Gros, P. (2000) *Biochemistry 39*, 4559−4568.
52. Wang, G., Pincheira, R., Zhang, M., and Zhang, J. T. (1997) *Biochem. J. 328*, 897−904.
53. Sankaran, B., Bhagat, S., and Senior, A. E. (1997) *Arch. Biochem. Biophys. 341*, 160−169.
54. Chen, J., Sharma, S., Quiocho, F. A., and Davidson, A. L. (2001) *Proc. Natl. Acad. Sci. U.S.A. 98*, 1525−1530.
55. Ramachandra, M., Ambudkar, S. V., Chen, D., Hrycyna, C. A., Dey, S., Gottesman, M. M., and Pastan, I. (1998) *Biochemistry 37*, 5010−5019.
56. Qu, Q., and Sharom, F. J. (2002) *Biochemistry*, in press.

BI026555J